World Journal of Engineering and Technology, 2015, 3, 84-88
Published Online October 2015 in SciRes. http://www.scirp.org/journal/wjet
http://dx.doi.org/10.4236/wjet.2015.33C013

Microstructure and Mechanical Properties of $NiTi_2$-TiB Composite Fabricated by Spark Plasma Sintering

Masashi Yoshida*, Hideo Shiraishi, Naoya Ikki

Department of Mechanical Engineering, Ube National College of Technology, Ube, Yamaguchi 755-8555, Japan
Email: *yoshida@ube-k.ac.jp

Received 9 August 2015; accepted 15 October 2015; published 22 October 2015

Abstract

Composites of $NiTi_2$-TiB have been fabricated using spark plasma sintering and mechanical properties have been investigated. Dense specimens of monolithic $NiTi_2$ have been obtained by the sintering at 950˚C. By the x-ray diffraction measurements it has been shown that $NiTi_2$ co-exists with TiB in equilibrium at 950˚C. The bending strength of $NiTi_2$-TiB composite increases with increasing the volume fraction of TiB_2 up to 60 vol%. The maximum bending strength of 730 MPa has been obtained for $NiTi_2$-60vol% TiB_2. The Vickers hardness also increases with increasing the volume fraction of TiB up to 70% and the highest Vickers hardness of 1620 Hv has been obtained for $NiTi_2$-70%TiB.

Keywords

Composite, Bending Strength, Vickers Hardness, TiB, $NiTi_2$

1. Introduction

There are three intermetallic compounds in the Ni-Ti system, Ni_3Ti, NiTi and $NiTi_2$, among which NiTi has received much interest for its shape memory effect [1]. $NiTi_2$ has favorable properties such as high corrosion resistance and wear resistance and Coating of Ti base alloys by $NiTi_2$ films has been examined [2]-[4]. On the other hand, bulk application of $NiTi_2$ has not been reported probably because of its poor ductility caused by the complicated E93-type lattice structure which contains 96 atoms in a unit cell [5].

The effective method to improve the mechanical properties is adding reinforcement components. Titanium boride (TiB) has many excellent properties such as high hardness (Vickers hardness, Hv, 16 GPa), high strength, high Young modulus (E = 371 GPa), low density (4.54 × 103 kg/m^3) and good corrosion resistance [6] [7]. It has needle like shape which is favorable for reinforcement materials [8]-[10].

In the present study we have fabricated monolithic $NiTi_2$ and $NiTi_2$-TiB composite by using Spark Plasma Sintering (SPS) method and investigated the Vickers hardness and bending strength. It has been shown that $NiTi_2$ is brittle and has poor fracture toughness which can be improved by the addition of TiB.

*Corresponding author.

How to cite this paper: Yoshida, M., Shiraishi, H. and Ikki, N. (2015) Microstructure and Mechanical Properties of NiTi2-TiB Composite Fabricated by Spark Plasma Sintering. *World Journal of Engineering and Technology*, **3**, 84-88.
http://dx.doi.org/10.4236/wjet.2015.33C013

2. Experimental Method

The raw materials were commercially available TiB_2, Ti and Ni powders of 99.9% purity (all powders by Furuuchi Chemical Corp.). The diameters of TiB_2, Ni, and Ti powder particles were 2 microns, 10 microns and 30 microns, respectively. TiB is formed from TiB_2 and Ti during the sintering by the reaction,

$$\mathrm{TIB_2 + Ti \rightarrow 2TiB} \quad (1)$$

A graphite die having an internal diameter of 20 mm and a wall thickness of 10 mm was filled with 5 g of the mixed powders of TiB_2, Ni and Ti and sealed by two graphite punches and mounted on the equipment, LABOX-630, fabricated by Sinter Land Ltd. The sintering temperature is determined as 950˚C since $NiTi_2$ melts peritectically at 984˚C. The mixed powders were heated to 950˚C with the rate of 50˚C/min, kept for 20 minutes, and then furnace cooled to room temperature. The temperature was measured using the infrared radiation thermometer IR-AHS0 fabricated by Chino Corporation. Sintering was performed in a vacuum with a residual pressure of 5 Pa. A uniaxial pressure of 20 MPa was applied during the sintering.

Scanning electron microscope (SEM) observation was performed using a Hitachi H-3300 instrument. X-ray diffraction patterns were measured using Rigaku X-ray diffract meter with Cu-kα radiation source. Vickers hardness was measured using a Shimadzu HMV-2 micro hardness tester with the load of 9.8 N and pressing time of 15 seconds. Five indentations are made to measure the length of indentation diagonals. To perform the bending test, rectangular shape samples with the size of 2 × 3 × 20 mm^3 were cut by the electric discharge. Three point bending tests were performed using a Shimadzu AGS-J test machine with the crosshead speed of 0.5 mm/min and the span of 15 mm. Four specimens ware measured for each composition.

3. Results and Discussion

Figure 1 shows the X-ray diffraction pattern of $NiTi_2$, $NiTi_2$-20vol%TiB, $NiTi_2$-40vol%TiB and $NiTi_2$-60volt% TiB specimens sintered at 950˚C. In the X-ray diffraction patterns of $NiTi_2$, peaks from cubic E93 type structure are observed. In the X-ray diffraction pattern of $NiTi_2$-TiB composites, peaks from TiB have been observed as indicated by arrows in addition to peaks from $NiTi_2$ showing that $NiTi_2$ and TiB co-exist in equilibrium at 950˚C. It should be noticed that no peaks from TiB2 is observed indicating that the chemical reaction of TiB2 and Ti have completed during the sintering process at 950˚C.

In **Figure 2** is shown the SEM images of the polished surface of (a) $NiTi_2$-40vol%TiB and (b) $NiTi_2$-70vol%TiB. In **Figure 2(a)**, it has been observed that dense samples are obtained with TiB grains of needle like shape dispersed in $NiTi_2$ matrix by the sintering at 950˚C. On the other hand, in **Figure 2(b)**, some cracks have been observed as indicated by arrows probably because of the thermal mismatch between TiB and $NiTi_2$.

We have performed the 3-point bending test and the Vickers hardness test to measure the mechanical properties of $NiTi_2$-TiB composites. In **Figure 3** is shown the dependence of the bending strength of $NiTi_2$-TiB composites on the amount of TiB. The bending strength of $NiTi_2$-10vol%TiB is 290 MPa, which increases as the amount of TiB increases up to 60% and the highest bending strength of 730 MPa has been obtained. The bending strength decreases as the amount of TiB increases above 60vol%. We could not measure the bending

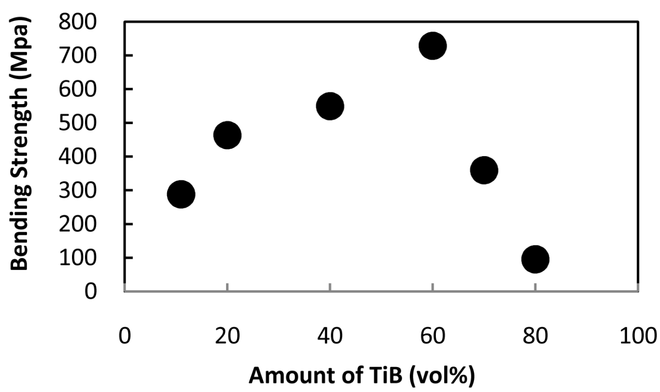

Figure 1. X-ray diffraction pattern from $NiTi_2$-TiB composites sintered at 950˚C.

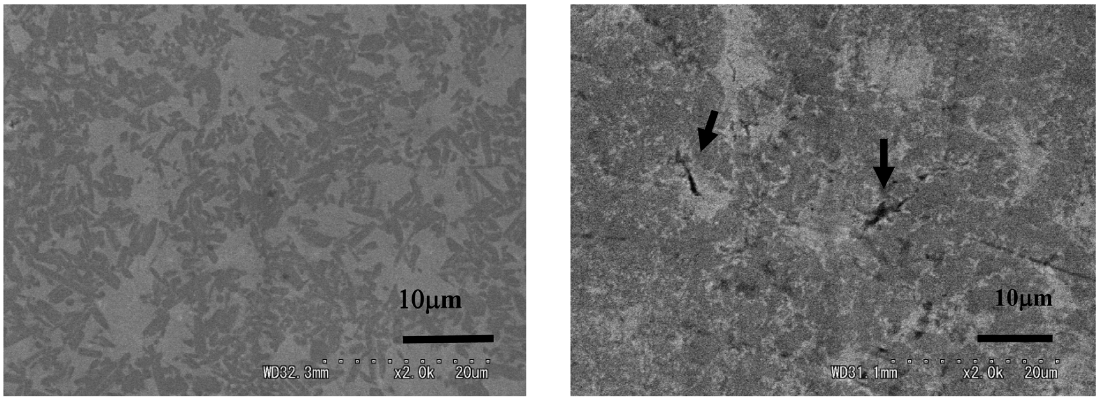

(a) (b)

Figure 2. SEM image of (a) $NiTi_2$-40vol%TiB and; (b) $NiTi_2$-70vol%TiB.

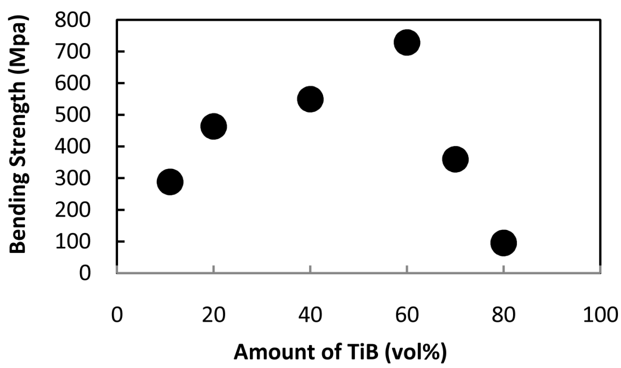

Figure 3. Bending strength of $NiTi_2$-TiB composites.

strength of monolithic $NiTi_2$ because $NiTi_2$ specimens have been cracked during the cutting procedure by using electric discharge. This decrease of the bending strength may be caused by the cracks as observed in **Figure 2(b)**.

Figure 4 shows the dependence of the Vickers hardness of $NiTi_2$-TiB composites on the amount of TiB. The Vickers hardness of $NiTi_2$ is 650 Hv. The Vickers hardness of $NiTi_2$ increases as the amount of TiB increases up to 70 vol% and decreases above 70%. The largest Hy value is 1620 Hv for $NiTi_2$-70vol%TiB specimen. .

Zhang et al. have fabricated Ti-TiB composite and investigated the bending strength and the Vickers hardness [11]. They have obtained the bending strength of 608 MPa and Vickers hardness of 18.3 GPa. The bending strength of NiTi2-TiB, 730 MPa, is higher than that of Ti-TiB composite while the Vickers hardness of NiTi2-TiB, 1620 Hv (15.9 GPa) is lower than that of Ti-TiB composite. This fact indicates that composites of intermetallics and ceramics are promising as well as metal-ceramics composites.

In **Figure 5** is shown the SEM images of the fracture surface of (a) $NiTi_2$, (b) $NiTi_2$-20vol%TiB and (c) $NiTi_2$-60vol%TiB and (d) $NiTi_2$-80vol%TiB. In **Figure 5(a)** it is shown that the fracture surface of $NiTi_2$ is composed by a few flat steps indicating that $NiTi_2$ has low fracture toughness. The fracture surface of $NiTi_2$-20wt%TiB contains several flat surface separated by TiB grains. It seems that the crack propagation is impeded by TiB grains. The dimension of the flat surface becomes smaller in the $NiTi_2$-60wt%TiB specimen in comparison with that of $NiTi_2$-20wt%TiB specimen, which may cause the improvement of the bending strength. In the fracture surface of $NiTi_2$-80vol% TiB specimen is observed granular regions where bonding between grains seems to be weak. The amount of $NiTi_2$ is not sufficient to fill the space between TiB grains in $NiTi_2$-80vol%TiB specimen.

4. Conclusion

Dense $NiTi_2$ and $NiTi_2$-TiB composite specimens have been fabricated using spark plasma sintering at 950˚C. The bending strength of $NiTi_2$-TiB increases as the amount of TiB increases up to 60% and the highest value of

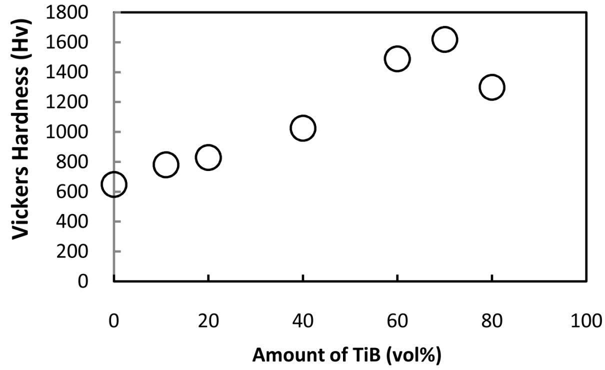

Figure 4. Vickers hardness of $NiTi_2$-TiB composites.

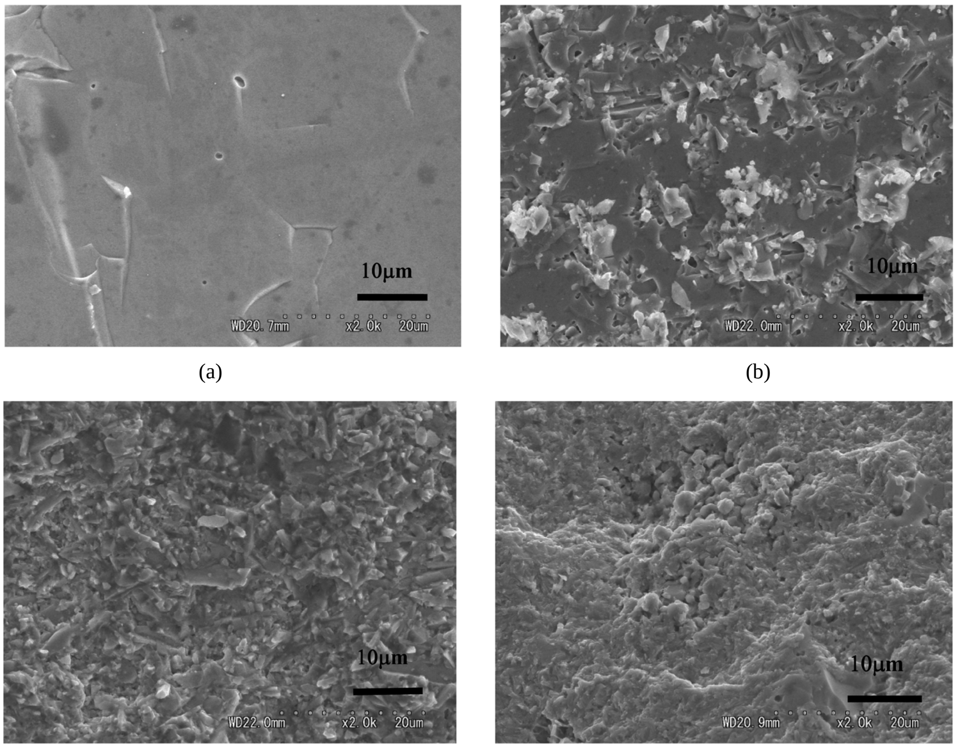

(a) (b) (c) (d)

Figure 5. Fracture surface of (a) $NiTi_2$; (b) $NiTi_2$-20%TiB; (c)$NiTi_2$-60%TiB and (d) $NiTi_2$-80%TiB.

730 MPa is obtained for $NiTi_2$-60vol%TiB. The Vickers hardness of monolithic $NiTi_2$ is 650 Hv, which increases up to 1620 for $NiTi_2$-60%TiB. In $NiTi_2$-TiB composite, crack propagation is observed to be impeded by TiB grains. Those values are nearly the same as those obtained for Ti-TiB composite and it has been shown that composites of intermetallics and ceramics are promising as well as metal-ceramics composites.

Acknowledgements

This work is supported by the Grant-in-Aid for Science Research from Japan Society for the promotion of Science (Kakenhi 25420739).

References

[1] Lagoudas, D.C. (2008) Shape Memory Alloys Modeling and Engineering Applications. Springer, Texas.

[2] Hiraga, H., Inoue, T., Shimura, H. and Matsunawa, A. (1999) Cavitation Erosion Mechanism of NiTi Coatings Made by Laser Plasma Hybrid Spraying. *Wear*, **231**, 272-278. http://dx.doi.org/10.1016/S0043-1648(99)00133-7

[3] Wang, H.W. and Liu, Y.F. (2002) Microstructure and Wear Resistance of Laser Clad Ti5Si3/NiTi2 Intermetallic Composite Coating on Titanium Alloy. *Materials Science and Engineering*: *A*, **338**, 126-132. http://dx.doi.org/10.1016/S0921-5093(02)00076-X

[4] Rampin, I., Brunelli, K., Dabala, M. and Magrini, M. (2009) Effect of Diffusion of Ni and B on the Microstructure and Hardness of Ti Cp. *Journal of Alloys and Compounds*, **481**, 246-253. http://dx.doi.org/10.1016/j.jallcom.2009.03.080

[5] Yurko, G.A., Barton, J.W. and Parr, J.G. (1959) The crystal structure of Ti_2Ni. *Acta Crystallographica*, **12**, 909-911. http://dx.doi.org/10.1107/S0365110X59002559

[6] Panda K.B. and Chandran, K.S.R. (2003) First Principles Determination of Elastic Constants and Chemical Bonding of Titanium Boride (TiB) on the Basis of Density Functional Theory. *Acta Materialia*, **54**, 1641-1657. http://dx.doi.org/10.1016/j.actamat.2005.12.003

[7] Atri, R.R., Ravichandran, K.S. and Jha, S.K. (1999) Elastic Properties of *in-Situ* Processed Ti-TiB Composition Measured by Impulse Excitation of Vibration. *Materials Science and Engineering*: *A*, **271**, 150-159. http://dx.doi.org/10.1016/S0921-5093(99)00198-7

[8] Gorsse, S., Petitcorps, Y.L., Matar, S. and Rebillat, F. (2003) Investigation of the Young's Modulus of TiB Needles *in Situ* Produced in Titanium Composite. *Materials Science and Engineering*: *A*, **340**, 80-87. http://dx.doi.org/10.1016/S0921-5093(02)00188-0

[9] Koo, M.Y., Park, J.S., Park, M.K., Kim, K.T. and Hong, S.H. (2012) Effect of Aspect Ratios of *in Situ* Formed TiB Whiskers on the Mechanical Properties of TiBw/Ti-6Al-4V Composites. *Scripta Materialia*, **66**, 487-490. http://dx.doi.org/10.1016/j.scriptamat.2011.12.024

[10] Shen, K., Zhang, Z., Wei, S., Wang, F. and Lee, S. (2011) Microstructure and Mechanical Properties of the *in Situ* TiB-Ti Metal Matrix Composites Synthesized by Spark Plasma Sintering Process. *Journal of Alloys and Compounds*, **509**, 7692-7696. http://dx.doi.org/10.1016/j.jallcom.2011.05.017

[11] Zhang, Z., Shen, X., Wen, S., Luo, J., Lee, S. and Wang, F. (2010) *In Situ* Reaction Synthesis of Ti-TiB Composites Containing High Volume Fraction of TiB by Spark Plasma Sintering Process. *Journal of Alloys and Compounds*, **503**, 145-150. http://dx.doi.org/10.1016/j.jallcom.2010.04.218